JACS
JOURNAL OF THE AMERICAN CHEMICAL SOCIETY
Article
pubs.acs.org/JACS

Three-Dimensional Covalent Organic Frameworks with Dual Linkages for Bifunctional Cascade Catalysis

Hui Li,[†,∥] Qinying Pan,[†,∥] Yunchao Ma,[†] Xinyu Guan,[†] Ming Xue,[†] Qianrong Fang,*[,†] Yushan Yan,[‡] Valentin Valtchev,[†,§] and Shilun Qiu*[,†]

[†]State Key Laboratory of Inorganic Synthesis and Preparative Chemistry, Jilin University, Changchun 130012, P. R. China
[‡]Department of Chemical and Biomolecular Engineering, Center for Catalytic Science and Technology, University of Delaware, Newark, Delaware 19716, United States
[§]Normandie Univ, ENSICAEN, UNICAEN, CNRS, Laboratoire Catalyse et Spectrochimie, 6 Marechal Juin, 14050 Caen, France

Supporting Information

ABSTRACT: Covalent organic frameworks (COFs) are an emerging class of porous crystalline polymers with broad potential applications. So far, the availability of three-dimensional (3D) COFs is limited and more importantly only one type of covalent bond has been successful used for 3D COF materials. Here, we report a new synthetic strategy based on dual linkages that leads to 3D COFs. The obtained 3D COFs show high specific surface areas and large gas uptake capacities, which makes them the top COF material for gas uptake. Furthermore, we demonstrate that the new 3D COFs comprise both acidic and basic sites, and act as excellent bifunctional catalysts for one-pot cascade reactions. The new synthetic strategy provides not only a general and versatile approach to synthesize 3D COFs with sophisticated structures but also expands the potential applications of this promising class of porous materials.

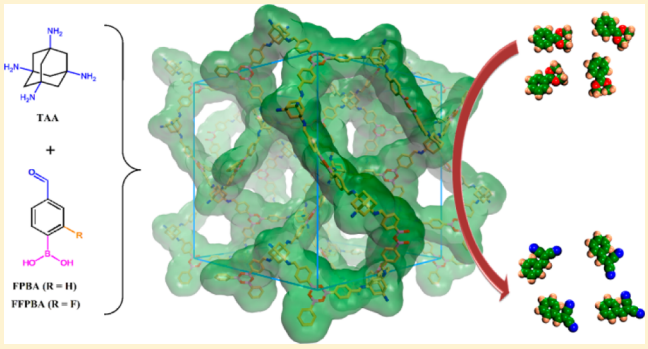

INTRODUCTION

Covalent organic frameworks (COFs),[1−4] as a new class of crystalline polymers, have attracted considerable attention over the past decade with promising performance in gas adsorption and separation,[5,6] catalysis,[7−9] optoelectronics,[10−13] proton conduction,[14,15] chemical sensing,[16,17] and drug delivery.[18,19] COFs are composed entirely of covalent bonds between light elements, typically H, B, C, N, and O, which crystallize into periodic architectures that can be precisely predetermined by the employed molecular building blocks. Since the pioneering work of Yaghi in 2005,[1] a variety of COFs have been prepared through several condensation reactions, including the formation of B−O (boronate, boroxine, and borosilicate),[20,21] B−N (borazine),[22] C−N (triazine and imide),[16,23] C═N (imine, hydrazine, and squaraine),[24−26] and N═N (azodioxide)[27] bond linkages. However, while the design and synthesis of 2D COFs is already well established,[28−32] the construction of 3D COFs is limited, and the successful synthetic methods for 3D COFs have been confined to only one type of covalent bond formation.[20,33] Thus, the exploration of a new synthetic strategy is of paramount importance for the development of 3D COF materials and diversifying their properties.

Herein we report a new general way to construct 3D COFs with the formation of two types of covalent bonds. On the basis of this strategy, two 3D COFs with dual linkages (boroxine and imine), denoted DL-COF-1 and DL-COF-2, were successfully obtained. Both materials show high surface areas and large gas storage capacities for H_2, CH_4 and CO_2. Furthermore, we demonstrate that both DL-COFs, consisting of both acidic and basic sites, can act as excellent bifunctional cascade catalysts. To the best of our knowledge, this study is the first example of 3D COFs with dual linkages and being applied to acid/base bifunctional catalysis.

RESULTS AND DISCUSSION

Our strategy for preparing 3D COFs with dual linkages involves the formation of imine group and boroxine ring. As shown in Scheme 1a, the condensation of 1-adamantanamine (AA) with 4-formylphenylboronic acid (FPBA) results in the triangular molecule with two kinds of covalent bonds. Through the same strategy, AA is replaced by an tetrahedral linker, 1,3,5,7-tetraaminoadamantane (TAA), which reacts with FPBA or 2-fluoro-4-formylphenylboronic acid (FFPBA) and thus produces two extended 3D framework structures, DL-COF-1 and DL-COF-2, respectively (Scheme 1b). In this case, tetrahedral TAA can be defined as a 4-connected node, and triangular boroxine ring can act as a 3-connected node. The association between

Received: September 12, 2016
Published: October 18, 2016

DOI: 10.1021/jacs.6b09563
J. Am. Chem. Soc. 2016, 138, 14783−14788

Scheme 1. Strategy for Preparing 3D COFs with Dual Linkages (DL-COFs)[a]

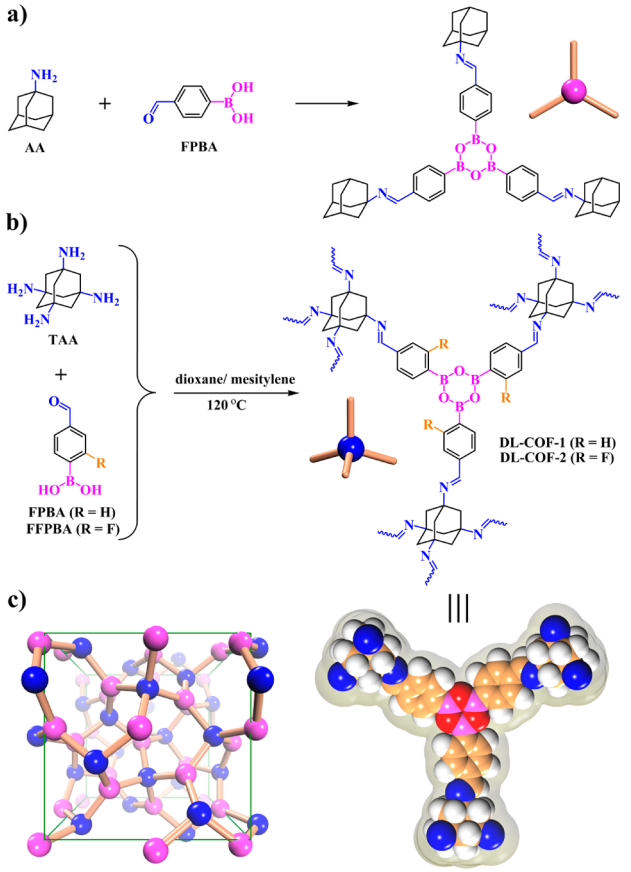

[a](a) Model reaction of 1-adamantanamine (AA) with 4-formylphenylboronic acid (FPBA) to form the triangular molecule with dual linkages. (b) Condensation of tetrahedral 1,3,5,7-tetraaminoadamantane (TAA) and FPBA or 2-fluoro-4-formylphenylboronic acid (FFPBA) to give 3D COFs with dual linkages, DL-COF-1 or DL-COF-2. (c) On the basis of triangular and tetrahedral building units, both DL-COFs show 3D networks with ctn topology.

the 3- and 4-connected building units results in 3D networks with the cubic carbon nitride (ctn) topology (Scheme 1c).[34]

The synthesis of DL-COFs was carried out by solvothermal reaction of TAA (9.8 mg, 0.05 mmol) and FPBA (30.0 mg, 0.2 mmol) or FFPBA (33.6 mg, 0.2 mmol) in a 1:1 (v:v) mixture of dioxane and mesitylene, followed by heating at 120 °C for 3 days. The yield of white crystalline solid was 82% for DL-COF-1 and 85% for DL-COF-2. These products were insoluble in common organic solvents such as tetrahydrofuran (THF), acetone, hexanes, *N*,*N*-dimethylformamide (DMF), dimethyl sulfoxide (DMSO), and *N*-methyl-2-pyrrolidone (NMP).

Scanning electron microscopy (SEM) study reveals that that both DL-COFs exhibit rectangular morphology with the particle size of about 0.2 μm (Figures S1 and S2). The crystals form random in size and morphology aggregates. Fourier transform infrared (FT-IR) spectra of DL-COFs (Figures S3 and S4) showed the disappearance of the hydroxyl stretching band (3215 cm^{-1} for FPBA and 3217 cm^{-1} for FFPBA), the carbonyl stretching band (1676 cm^{-1} for FPBA and 1684 cm^{-1} for FFPBA), and the N−H stretching band (around 3300 cm^{-1}) of TAA, indicating a completed conversion of these groups. Meanwhile, the characteristic stretching bands of the imine group (1644 cm^{-1} for DL-COF-1 and 1641 cm^{-1} for DL-COF-2) and the B−O and B_3O_3 ring (715, 1297, and 1336 cm^{-1} for DL-COF-1 and 717, 1303, and 1340 cm^{-1} for DL-COF-2) emerged in the IR spectra.[1,30] These data unambiguously show that the structures of the new COFs are built of networks with dual linkages. The atomic precision construction of DL-COFs was further verified by the ^{13}C cross-polarization magic-angle-spinning (CP/MAS) NMR spectroscopy (Figures S5 and S6) that confirmed the presence of carbonyl carbon from the imide ring at 168 ppm for DL-COF-1 and 166 ppm for DL-COF-2. The structure of DL-COFs, built up of dual covalent linkages, showed high thermal stability. According to the thermogravimetric analysis (TGA) the DL-COFs are stable up to 400 °C (Figures S7 and S8).

The crystalline nature of both DL-COFs was confirmed by powder X-ray diffraction (PXRD) analysis (Figure 1). After a

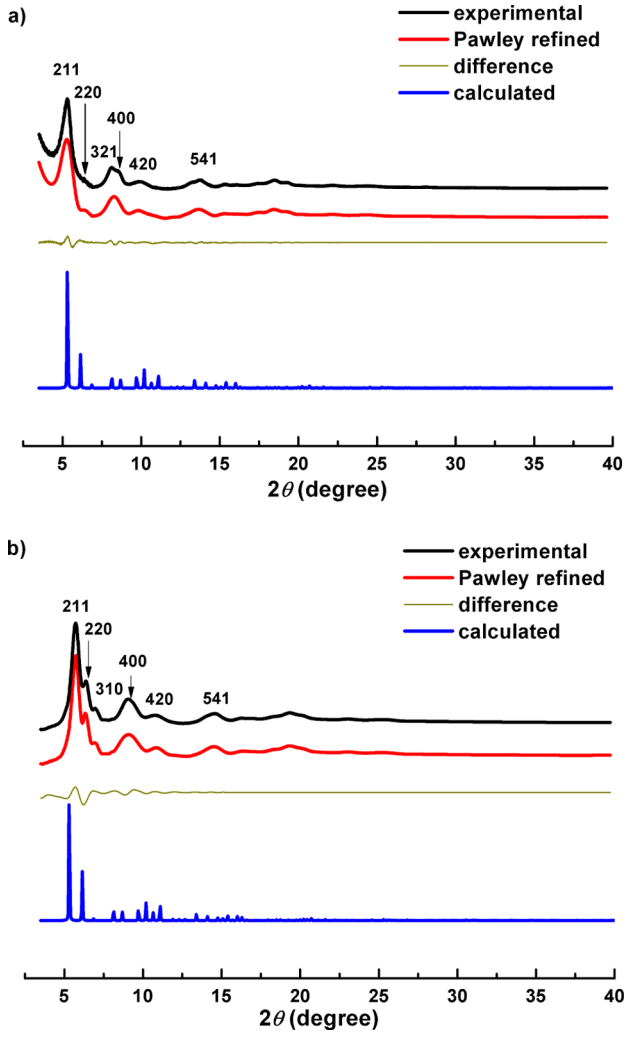

Figure 1. PXRD patterns of DL-COF-1 (a) and DL-COF-2 (b) with the observed profile in black, refined in red, the difference (observed minus refined) in dark yellow, and calculated based on the ctn topology in blue.

geometrical energy minimization by using the Materials Studio Software package[35] based on the ctn topology the unit cell parameters were determined. Both materials exhibit cubic unit cells with $a = b = c = 41.0115$ Å and $\alpha = \beta = \gamma = 90°$ for DL-COF-1; and $a = b = c = 41.0142$ Å and $\alpha = \beta = \gamma = 90°$ for DL-COF-2. Simulated PXRD patterns show good match with the

DOI: 10.1021/jacs.6b09563
J. Am. Chem. Soc. 2016, 138, 14783−14788

experimental ones (Figure 1, black and blue curves). Furthermore, the full profile pattern matching (Pawley) refinements are performed from the experimental PXRD patterns. Strong PXRD peaks at 5.30, 6.15, 8.10, 8.71, 10.20, and 13.40° for DL-COF-1 can be assigned to the (211), (220), (321), (400), (420), and (541) Bragg peaks of $I\bar{4}3d$ (No. 220); and 5.30, 6.15, 6.85, 8.71, 10.20 and 13.40° for DL-COF-2 correspond to the (211), (220), (310), (400), (420), and (541) Bragg peaks of $I\bar{4}3d$ (No. 220), respectively. The refinement results revealed unit cell parameters nearly equivalent to the predictions with excellent agreement factors ($a = b = c = 40.8123$ Å, $\alpha = \beta = \gamma = 90°$, $wR_p = 3.21\%$, and $R_p = 1.73\%$ for DL-COF-1; $a = b = c = 40.8324$ Å, $\alpha = \beta = \gamma = 90°$, $wR_p = 3.03\%$, and $R_p = 1.66\%$ for DL-COF-2). Besides the ctn network, we also considered alternative topologies based on the boracite (bor) net, which were set up from the space groups of $P23$ (No. 195). However, these calculated patterns did not match the experimental PXRD patterns (Figures S9−14 and Tables S1−4). On the basis of the above results, both DL-COFs were proposed to have the expected architectures with the ctn topology, which show microporous cavities with a diameter of about 14.2 Å (Figure 2).

The porosity of DL-COFs was demonstrated by measuring nitrogen-gas (N_2) adsorption at 77 K. As can be seen in Figure 3, both DL-COFs exhibit the characteristic for microporous materials type I isotherm with sharp uptake below 0.1 P/P_0. The inclination of the isotherm in the 0.1−1.0 P/P_0 range reveals the presence of textural mesopores, which are a consequence of the agglomeration of nanosized COF crystals (Figures S1 and S2). The lack of hysteresis indicates that the adsorption and desorption mechanisms are similar and that the adsorption is reversible. The application of the Brunauer−Emmett−Teller (BET) model in the low pressure region ($0.005 < P/P_0 < 0.07$) showed a specific surface areas of 2259 $m^2\ g^{-1}$ for DL-COF-1 and 2071 $m^2\ g^{-1}$ for DL-COF-2 (Figures S15 and S16). The pore-size distributions of DL-COFs were calculated by nonlocal density functional theory (NLDFT). Both DL-COFs showed a narrow pore width (13.6 Å for DL-COF-1 and 12.8 Å for DL-COF-2, Figures S17 and S18), which was in good agreement with the pore size predicted from their crystal structures (14.2 Å for both DL-COFs).

Because of the high BET surface area of DL-COFs, hydrogen (H_2), carbon dioxide (CO_2) and methane (CH_4) adsorption was also studied to explore their potential application in gas storage (Figure 4). The gas adsorption isotherms were collected at 77 K for H_2, and 273 K for CO_2 and CH_4. At 1.0 bar, DL-COF-1 shows uptake as high as 234 $cm^3\ g^{-1}$ (2.09 wt %) of H_2, 136 $cm^3\ g^{-1}$ (26.7 wt %) of CO_2, and 36 $cm^3\ g^{-1}$ (2.57 wt %) of CH_4. Similarly, at 1.0 bar, DL-COF-2 can store up to 193 $cm^3\ g^{-1}$ (1.73 wt %) of H_2, 111 $cm^3\ g^{-1}$ (21.8 wt %) of CO_2, and 30 $cm^3\ g^{-1}$ (2.10 wt %) of CH_4. These results are among the highest values for COFs, such as NTU-COF-2 (1.55 wt % of H_2),[30] TDCOF-5 (1.6 wt % of H_2),[36] TpPa-COF (21.8 wt % of CO_2),[37] and FCTF-1-600 (24.4 wt % of CO_2),[38] which places DL-COFs among the top COF material for gas uptake.

Encouraged by high crystallinity and porosity as well as by the proximity of acidic and basic catalytic sites of DL-COFs, we have explored the catalytic potential of new COFs for the acid−base catalyzed one-pot cascade reactions. Up to now, only a 2D catechol-porphyrin COF with a single type linkage was used for a bifunctional catalytic reaction.[39] To the best of our knowledge, such exploration has not been extended to 3D COF materials. Compared with 2D COFs, 3D COF materials possess interrelated porous structures and higher specific surface areas, which are key characteristics those allow a heterogeneous catalyst to achieve high activity. Hence, the 3D COFs are expected to be a promising bifunctional catalyst. In this work, the employed reaction involves hydrolysis of the acetal catalyzed by the acidic sites of boroxine group followed by Knoevenagel condensation catalyzed by the basic sites of imine bonds (Scheme 2).

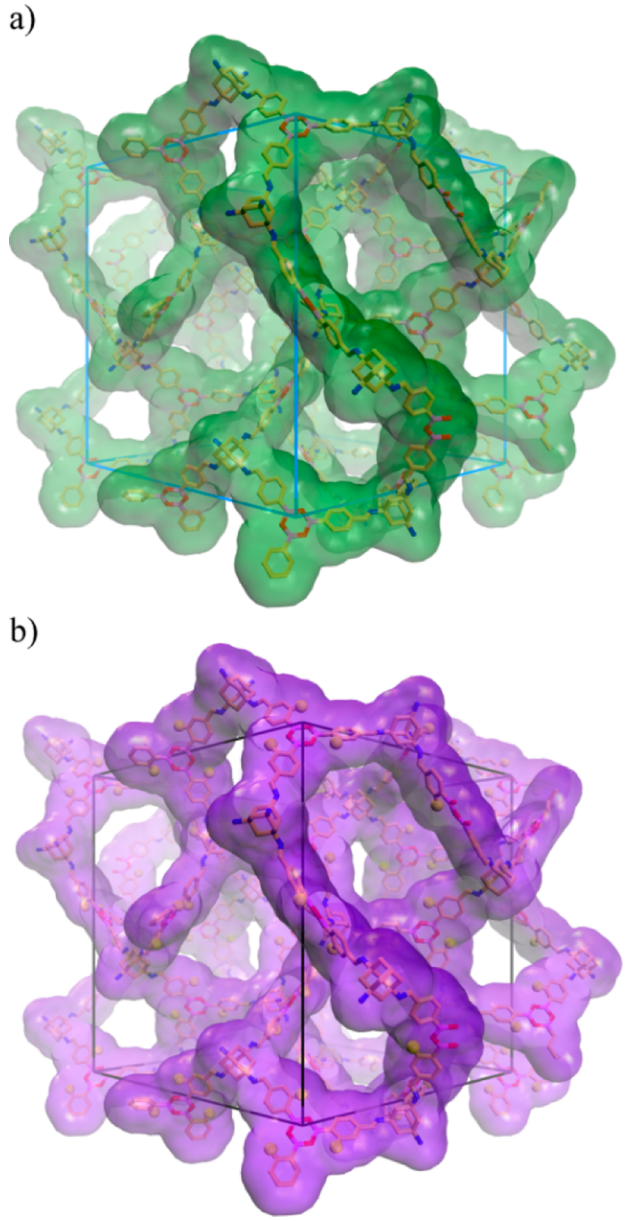

Figure 2. Structural representations of 3D DL-COF-1 (a) and DL-COF-2 (b).

Typically, the catalytic reaction was performed with 1 mmol of each reactant in $CDCl_3$ (3 mL) with DL-COF-1 or DL-COF-2 (10 mol %) at room temperature for 20 h. The conversion and the product distribution were monitored by ^1H NMR spectroscopy based on the starting materials. As shown in Scheme 2, reactant A (benzaldehyde dimethyl acetal) was hydrolyzed to give product B (benzaldehyde), which further reacted with C (malononitrile, ethyl cyanoacetate, or acetylacetone) to form the final product D (benzylidene malononitrile, ethyl *trans*-α-cyanocinnamate, or 3-benzylidene-

DOI: 10.1021/jacs.6b09563
J. Am. Chem. Soc. 2016, 138, 14783−14788

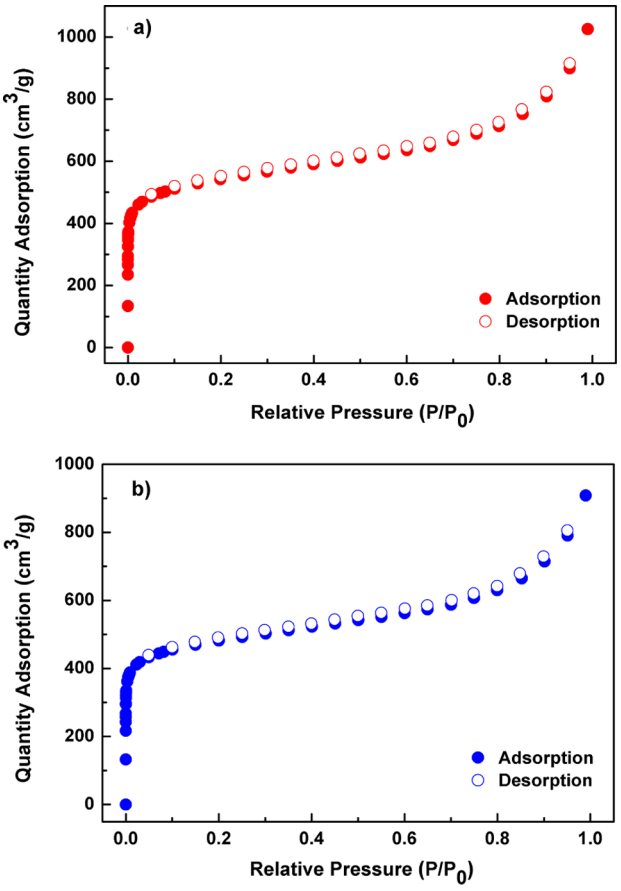

Figure 3. N_2 adsorption−desorption isotherms for DL-COF-1 (a) and DL-COF-2 (b) at 77 K.

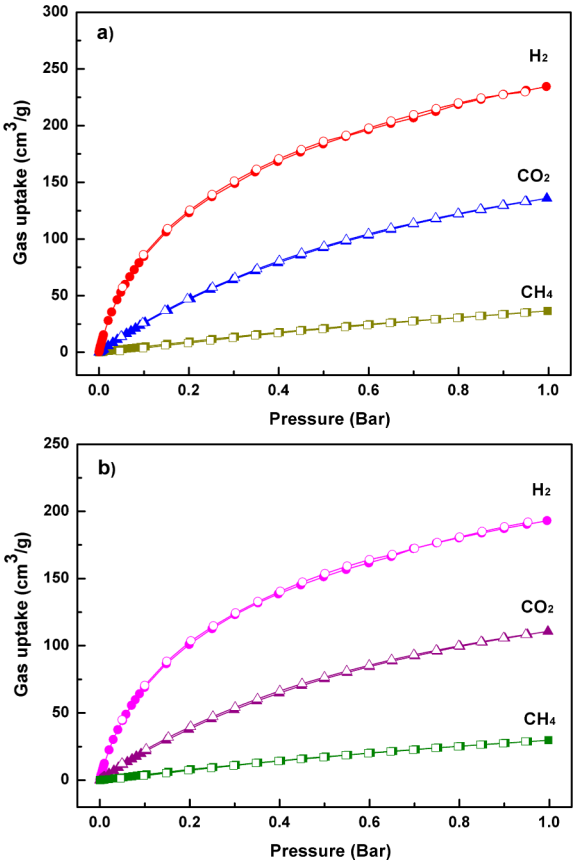

Figure 4. H_2, CO_2 and CH_4 adsorption isotherms of DL-COF-1 (a) and DL-COF-2 (b). Filled and empty symbols represent the adsorption and desorption branches, respectively.

2,4-pentanedione). As mentioned, the first reaction step requires acidic sites, which are supplied by boroxine group, whereas the subsequent condensation step involves the basic sites from imine bonds in DL-COFs. Figure 5 shows the conversion of benzaldehyde dimethyl acetal (100%) and the formation of benzaldehyde intermediate that is reacted through consecutive Knoevenagel condensation with malononitrile to give the final product, benzylidene malononitrile (98% for DL-COF-1 and 96% for DL-COF-2). Furthermore, by replacing malononitrile reactant with ethyl cyanoacetate or acetylacetone, and keeping all other reaction conditions the same, similar results can be obtained (Scheme 2 and Figures S19−S22). After the reactions, the results of PXRD and N_2 adsorption confirmed the structural integrity of DL-COFs, thus revealing the high stability of new COF materials in the acid−base catalytic reaction (Figures S23−S26). The COF crystals can be easily isolated from the reaction mixture by a simple filtration and reused at least three times with almost no loss of activity (Figures S27 and S28).

CONCLUSIONS

In conclusion, we have developed a new strategy to construct 3D COFs by employing two types of covalent bonds. Two novel 3D COFs with both boroxine and imine dual linkages were for the first time prepared, and showed large surface areas as well as high H_2, CH_4 and CO_2 uptake capacities. In addition, we explored the catalytic activity of new COF materials, comprising both acidic and basic sites, in acid−base catalyzed one-pot cascade reactions. 3D bifunctional COF catalysts

Scheme 2. Catalytic Activity of DL-COFs in Acid−Base Catalyzed One-Pot Cascade Reactions

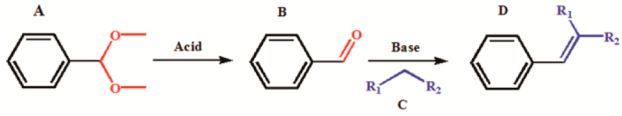

Entry	Catalyst	C	Conversion of D (%)
1	DL-COF-1	$R_1 = R_2 = CN$	98
2	DL-COF-2	$R_1 = R_2 = CN$	96
3	DL-COF-1	$R_1 = CN$, $R_2 = COOC_2H_5$	93
4	DL-COF-2	$R_1 = CN$, $R_2 = COOC_2H_5$	92
5	DL-COF-1	$R_1 = R_2 = COCH$	93
6	DL-COF-2	$R_1 = R_2 = COCH$	94

successfully prepared in this work may not only expand the development of COFs with more sophisticated structures and compositions, but also promote the applications of COFs as multifunctional materials.

EXPERIMENTAL SECTION

Starting Materials. All starting materials and solvents, unless otherwise noted, were obtained from J&K scientific Ltd. and used without purification. 1,3,5,7-Tetraaminoadamantane (TAA) was synthesized by the method in literature.[8]

Synthesis of DL-COF-1. A Pyrex tube measuring o.d. × i.d. = 10 × 8 mm^2 was charged with FPBA (30.0 mg, 0.2 mmol) and TAA (9.8 mg, 0.05 mmol) in a mixed solution of dioxane (0.5 mL) and mesitylene (0.5 mL). The tube was flash frozen at 77 K (LN_2 bath),

DOI: 10.1021/jacs.6b09563
J. Am. Chem. Soc. 2016, 138, 14783−14788

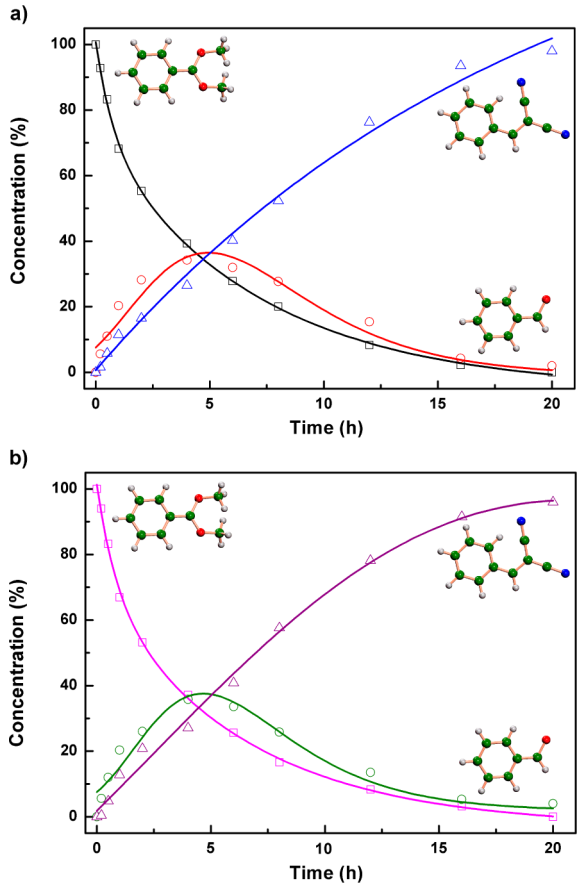

Figure 5. Conversion (%) versus time (h) for bifunctional catalytic reactions on DL-COF-1 (a) and DL-COF-2 (b) based on entry 1 and 2 in Scheme 2, respectively. Inset: structures of reactant, intermediate, and final product. H, gray; C, green; N, blue; O, red.

evacuated to an internal pressure of 0.15 mmHg, and flame-sealed. Upon sealing, the length of the tube was reduced to ca. 13 cm. The reaction mixture was heated at 120 °C for 3 days to afford a white precipitate which was isolated by filtration over a medium glass frit and washed with anhydrous tetrahydrofuran (THF, 20.0 mL). The product was immersed in anhydrous THF (20.0 mL) for 8 h, during which the activation solvent was decanted and freshly replenished four times. The solvent was removed under vacuum at 80 °C to afford DL-COF-1 as a white powder (26.7 mg, 82%).

Synthesis of DL-COF-2. Similar to DL-COF-1, FPBA was treated with FFPBA (33.6 mg, 0.2 mmol) in a mixed solution of dioxane (0.5 mL) and mesitylene (0.5 mL). The tube was flash frozen at 77 K (LN_2 bath), evacuated to an internal pressure of 0.15 mmHg, and flame-sealed. Upon sealing, the length of the tube was reduced to ca. 13 cm. The reaction mixture was heated at 120 °C for 3 days to afford a white precipitate which was isolated by filtration over a medium glass frit and washed with anhydrous THF (20.0 mL). The product was immersed in anhydrous THF (20.0 mL) for 8 h, during which the activation solvent was decanted and freshly replenished four times. The solvent was removed under vacuum at 80 °C to afford DL-COF-2 as a white powder (30.9 mg, 85%).

Further detailed experimental procedures and characterization are described in the Supporting Information.

■ ASSOCIATED CONTENT

Supporting Information

The Supporting Information is available free of charge on the ACS Publications website at DOI: 10.1021/jacs.6b09563.

Synthetic procedures, SEM, FTIR, solid state ^{13}C NMR, TGA, BET plot, and pore size distribution (PDF)

■ AUTHOR INFORMATION

Corresponding Authors

*qrfang@jlu.edu.cn

*sqiu@jlu.edu.cn

Author Contributions

‖H.L. and Q.P. contributed equally to this work.

Notes

The authors declare no competing financial interest.

■ ACKNOWLEDGMENTS

This work was supported by National Natural Science Foundation of China (21390394, 21261130584, 21571079, and 21571076), "111" Project (B07016), Guangdong Science and Technology Department Project (2009B090300432), and Ministry of Education, Science and Technology Development Center Project (20120061130012). V.V. and Q.F. acknowledge the Thousand Talents program (China).

■ REFERENCES

(1) Côté, A. P.; Benin, A. I.; Ockwig, N. W.; O'Keeffe, M.; Matzger, A. J.; Yaghi, O. M. *Science* **2005**, *310*, 1166.

(2) Colson, J. W.; Woll, A. R.; Mukherjee, A.; Levendorf, M. P.; Spitler, E. L.; Shields, V. B.; Spencer, M. G.; Park, J.; Dichtel, W. R. *Science* **2011**, *332*, 228.

(3) Feng, X.; Ding, X.; Jiang, D. *Chem. Soc. Rev.* **2012**, *41*, 6010.

(4) Ding, S. Y.; Wang, W. *Chem. Soc. Rev.* **2013**, *42*, 548.

(5) Furukawa, H.; Yaghi, O. M. *J. Am. Chem. Soc.* **2009**, *131*, 8875.

(6) Han, S. S.; Mendoza-Cortes, J. L.; Goddard, W. A., III *Chem. Soc. Rev.* **2009**, *38*, 1460.

(7) Ding, S. Y.; Gao, J.; Wang, Q.; Zhang, Y.; Song, W. G.; Su, C. Y.; Wang, W. *J. Am. Chem. Soc.* **2011**, *133*, 19816.

(8) Fang, Q. R.; Gu, S.; Zheng, J.; Zhuang, Z. B.; Qiu, S. L.; Yan, Y. S. *Angew. Chem., Int. Ed.* **2014**, *53*, 2878.

(9) Xu, H.; Gao, J.; Jiang, D. L. *Nat. Chem.* **2015**, *7*, 905.

(10) Wan, S.; Guo, J.; Kim, J.; Ihee, H.; Jiang, D. *Angew. Chem., Int. Ed.* **2008**, *47*, 8826.

(11) Bertrand, G. H. V.; Michaelis, V. K.; Ong, T. C.; Griffin, R. G.; Dinca, M. *Proc. Natl. Acad. Sci. U. S. A.* **2013**, *110*, 4923.

(12) Dogru, M.; Bein, T. *Chem. Commun.* **2014**, *50*, 5531.

(13) Liu, X. H.; Guan, C. Z.; Wang, D.; Wan, L. J. *Adv. Mater.* **2014**, *26*, 6912.

(14) Chandra, S.; Kundu, T.; Kandambeth, S.; BabaRao, R.; Marathe, Y.; Kunjir, S. M.; Banerjee, R. *J. Am. Chem. Soc.* **2014**, *136*, 6570.

(15) Xu, H.; Tao, S. S.; Jiang, D. L. *Nat. Mater.* **2016**, *15*, 722.

(16) Fang, Q. R.; Zhuang, Z. B.; Gu, S.; Kaspar, R. B.; Zheng, J.; Wang, J. H.; Qiu, S. L.; Yan, Y. S. *Nat. Commun.* **2014**, *5*, 4503.

(17) Das, G.; Biswal, B. P.; Kandambeth, S.; Venkatesh, V.; Kaur, G.; Addicoat, M.; Heine, T.; Verma, S.; Banerjee, R. *Chem. Sci.* **2015**, *6*, 3931.

(18) Fang, Q. R.; Wang, J. H.; Gu, S.; Kaspar, R. B.; Zhuang, Z. B.; Zheng, J.; Guo, H. X.; Qiu, S. L.; Yan, Y. S. *J. Am. Chem. Soc.* **2015**, *137*, 8352.

(19) Bai, L. Y.; Phua, S. Z. F.; Lim, W. Q.; Jana, A.; Luo, Z.; Tham, H. P.; Zhao, L. Z.; Gao, Q.; Zhao, Y. L. *Chem. Commun.* **2016**, *52*, 4128.

(20) El-Kaderi, H. M.; Hunt, J. R.; Mendoza-Cortés, J. L.; Côté, A. P.; Taylor, R. E.; O'Keeffe, M.; Yaghi, O. M. *Science* **2007**, *316*, 268.

(21) Hunt, J. R.; Doonan, C. J.; LeVangie, J. D.; Côté, A. P.; Yaghi, O. M. *J. Am. Chem. Soc.* **2008**, *130*, 11872.

(22) Jackson, K. T.; Reich, T. E.; El-Kaderi, H. M. *Chem. Commun.* **2012**, *48*, 8823.

(23) Kuhn, P.; Antonietti, M.; Thomas, A. *Angew. Chem., Int. Ed.* **2008**, *47*, 3450.

DOI: 10.1021/jacs.6b09563
J. Am. Chem. Soc. 2016, 138, 14783−14788

(24) Uribe-Romo, F. J.; Hunt, J. R.; Furukawa, H.; Klöck, C.; O'Keeffe, M.; Yaghi, O. M. *J. Am. Chem. Soc.* **2009**, *131*, 4570.
(25) Uribe-Romo, F. J.; Doonan, C. J.; Furukawa, H.; Oisaki, K.; Yaghi, O. M. *J. Am. Chem. Soc.* **2011**, *133*, 11478.
(26) Nagai, A.; Chen, X.; Feng, X.; Ding, X.; Guo, Z.; Jiang, D. L. *Angew. Chem., Int. Ed.* **2013**, *52*, 3770.
(27) Beaudoin, D.; Maris, T.; Wuest, J. D. *Nat. Chem.* **2013**, *5*, 830.
(28) Colson, J. W.; Dichtel, W. R. *Nat. Chem.* **2013**, *5*, 453.
(29) Zhu, Y. L.; Wan, S.; Jin, Y. H.; Zhang, W. *J. Am. Chem. Soc.* **2015**, *137*, 13772.
(30) Zeng, Y. F.; Zou, R. Y.; Luo, Z.; Zhang, H. C.; Yao, X.; Ma, X.; Zou, R. Q.; Zhao, Y. L. *J. Am. Chem. Soc.* **2015**, *137*, 1020.
(31) Chen, X.; Addicoat, M.; Jin, E. Q.; Xu, H.; Hayashi, T.; Xu, F.; Huang, N.; Irle, S.; Jiang, D. L. *Sci. Rep.* **2015**, *5*, 14650.
(32) Du, Y.; Yang, H. S.; Whiteley, J. M.; Wan, S.; Jin, Y. H.; Lee, S. H.; Zhang, W. *Angew. Chem., Int. Ed.* **2016**, *55*, 1737.
(33) Lin, G. Q.; Ding, H. M.; Yuan, D. Q.; Wang, B. S.; Wang, C. *J. Am. Chem. Soc.* **2016**, *138*, 3302.
(34) Delgado-Friedrichs, O.; O'Keeffe, M.; Yaghi, O. M. *Acta Crystallogr., Sect. A: Found. Crystallogr.* **2006**, *62*, 350.
(35) *Materials Studio ver. 7.0*; Accelrys Inc.: San Diego, CA.
(36) Kahveci, Z.; Islamoglu, T.; Shar, G. A.; Ding, R.; El-Kaderi, H. M. *CrystEngComm* **2013**, *15*, 1524.
(37) Wei, H.; Chai, S.; Hu, N.; Yang, Z.; Wei, L.; Wang, L. *Chem. Commun.* **2015**, *51*, 12178.
(38) Zhao, Y.; Yao, K. X.; Teng, B.; Zhang, T.; Han, Y. *Energy Environ. Sci.* **2013**, *6*, 3684.
(39) Shinde, D. B.; Kandambeth, S.; Pachfule, P.; Kumar, R. R.; Banerjee, R. *Chem. Commun.* **2015**, *51*, 310.

DOI: 10.1021/jacs.6b09563
J. Am. Chem. Soc. 2016, 138, 14783−14788